Cell Reports, Volume *38*

Supplemental information

CDC42 controlled apical-basal polarity regulates intestinal stem cell to transit amplifying cell fate transition via YAP-EGF-mTOR signaling

Zheng Zhang, Feng Zhang, Ashley Kuenzi Davis, Mei Xin, Gerd Walz, Weidong Tian, and Yi Zheng

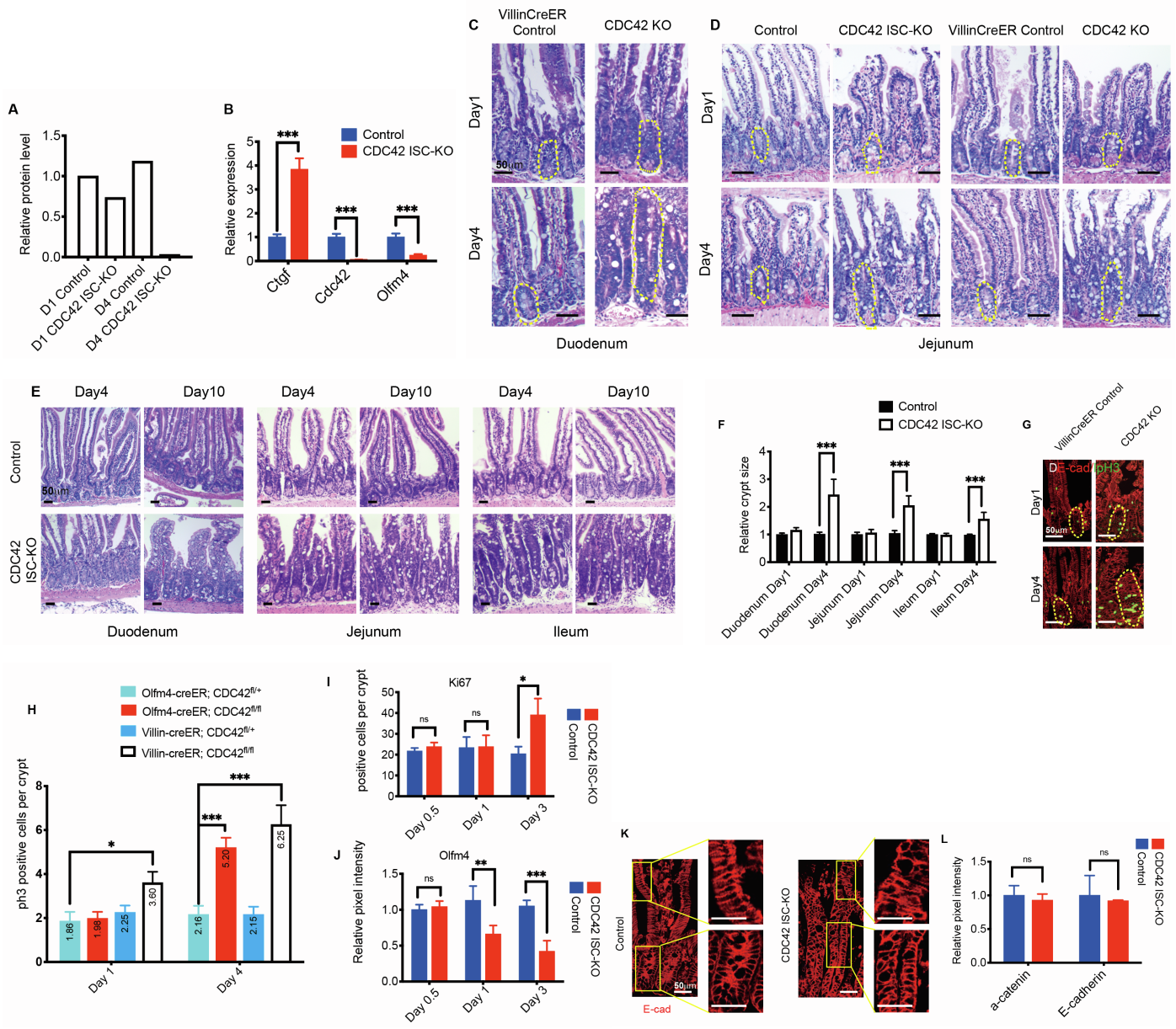

Supplemental Figure 1. ISC-specific deletion of CDC42 mimics whole epithelium deletion in duodenum and ileum, and disrupts crypt structure.

Related to Figure 1

(A) Quantification of Fig. 1A Western Blotting.

(B) Relative mRNA levels of Ctgf, CDC42 and Olfm4 in sorted GFP+ (ISCs) cells and GFP- (non-ISCs) from isolated small intestinal crypts. Data are mean ± SD; ***p < 0.005.

(C) Representative images of H&E staining of duodenal sections; 1 crypt circled in each image.

(D) Representative images of H&E staining of jejunal sections; 1 crypt circled in each image.

(E) Representative images of H&E staining of duodenal, jejunal and ileal sections;

(F) Quantification of relative crypt size. Data are mean ± SD; ***p < 0.005.

(G) Representative images of immunofluorescent staining of duodenal sections: E-cadherin and pH3; One representative crypt circled in each sample.

(H) Quantification of ph3 positive cells per crypt. Data are mean ± SD; *p < 0.05; ***p < 0.005.

(I) Quantification of Ki67 positive cells per crypt in Fig. 1H, I. Data are mean ± SD; *p < 0.05; ns: not significant.

(J) Quantification of Olfm4 staining Fig. 1J, K. Data are mean ± SD; ns: not significant, **p < 0.01; ***p < 0.005.

(K) Representative images of immunofluorescent staining of duodenal sections: E-cadherin; enlargements of villi (‘) and crypt (‘’).

(L) Quantification of a-catenin and E-cadherin. Data are mean ± SD; ns: not significant.

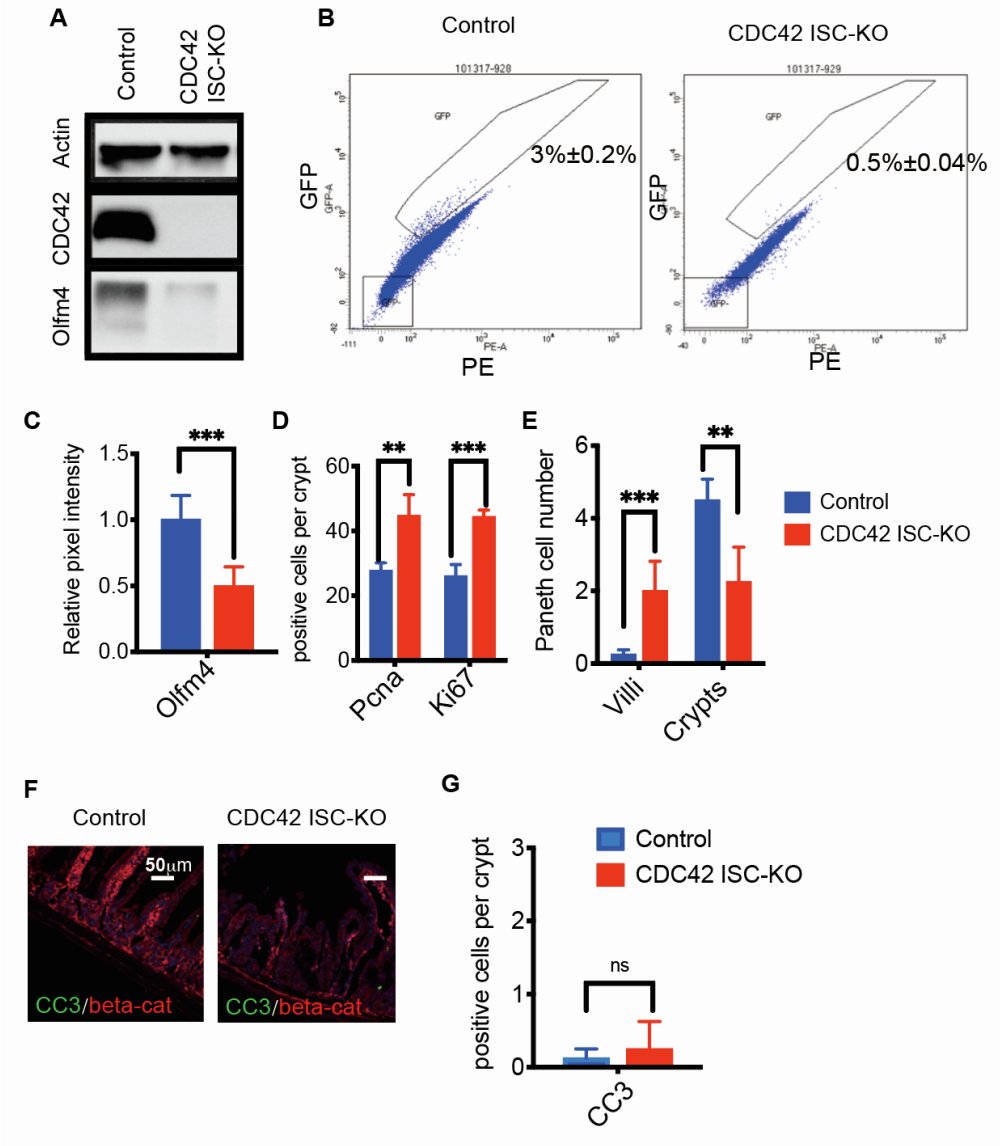

Supplemental Figure 2. Loss of CDC42 in ISCs decreases ISCs without causing ectopic apoptosis. Related to Figure 2

(A) Western Blotting of CDC42 and Olfm4 in isolated small intestinal crypts.

(B) Flow cytometry of Olfm4-eGFP positive cells in suspended single cells from isolated small intestinal crypts.

(C-E) Quantification of immunofluorescent staining in Fig. 2B-E. Data are mean ± SD. **p < 0.01; ***p < 0.005.

(F) Representative images of immunofluorescent staining of duodenal sections: active caspase 3.

(G) Quantification of active caspase 3 positive cells per crypt. Data are mean ± SD; ns: not significant.

A

	Control	CDC42 ISC-KO	YAP KO/ TAZ het rescue
ISCs (Lgr5)	5.68%	0.42%	3.17%
TA cells (Pcna)	16.56%	25.03%	29.21%

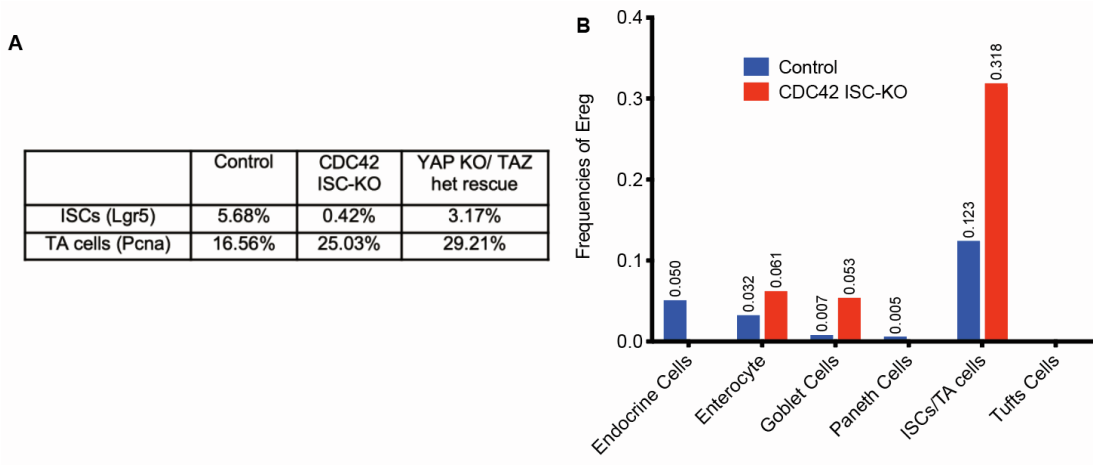

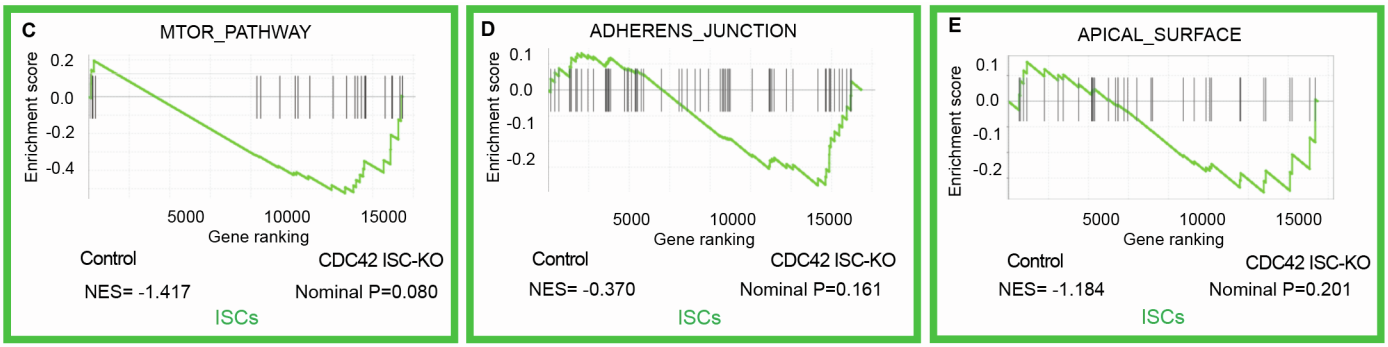

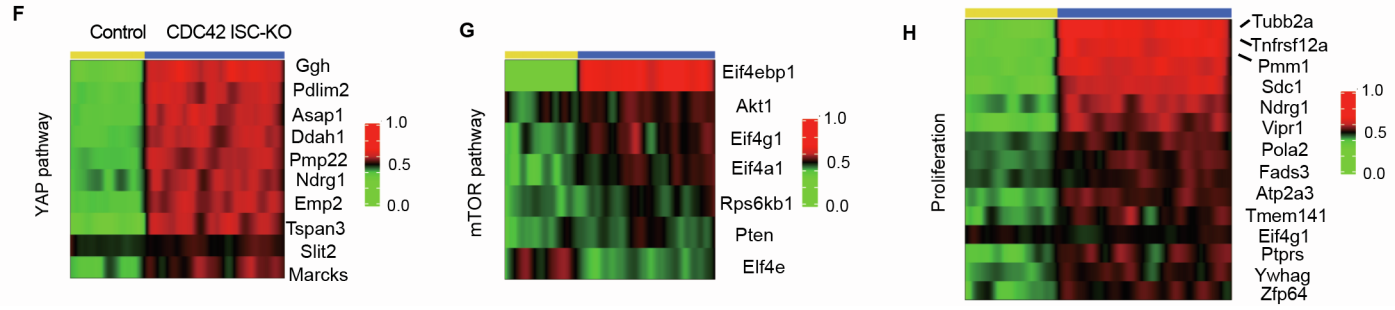

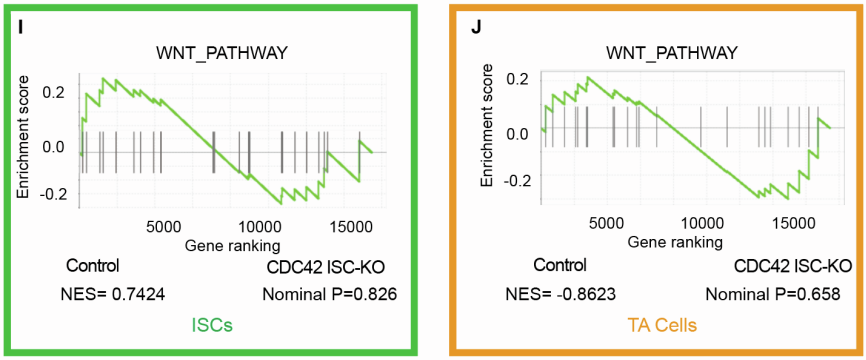

Supplemental Figure 3. Activity of mTOR, apical surface and adhesion junction pathways are increased in CDC42-depleted ISCs, while canonical Wnt is un-altered in both ISCs and TA cells. **Related to Figure 3**

(A) Percentage of ISC marker (Lgr5) and TA cell marker (Pcna) in scRNAseq analysis.

(B) Positive frequencies of Ereg in each cell clusters.

(C-E) GSEA pathway enrichment map for mTOR, apical polarity, and adhesion junction pathways in ISC cluster.

(F-H) Heatmap of most-differentially altered genes in YAP pathway (10 genes), mTOR pathway (7 genes), and proliferation pathways (14 genes) in control and CDC42 ISC-KO TA cell cluster. Columns, individual cells; rows, genes. n refers to gene numbers.

(I, J) GSEA pathway enrichment map for canonical Wnt in ISCs and TA clusters.

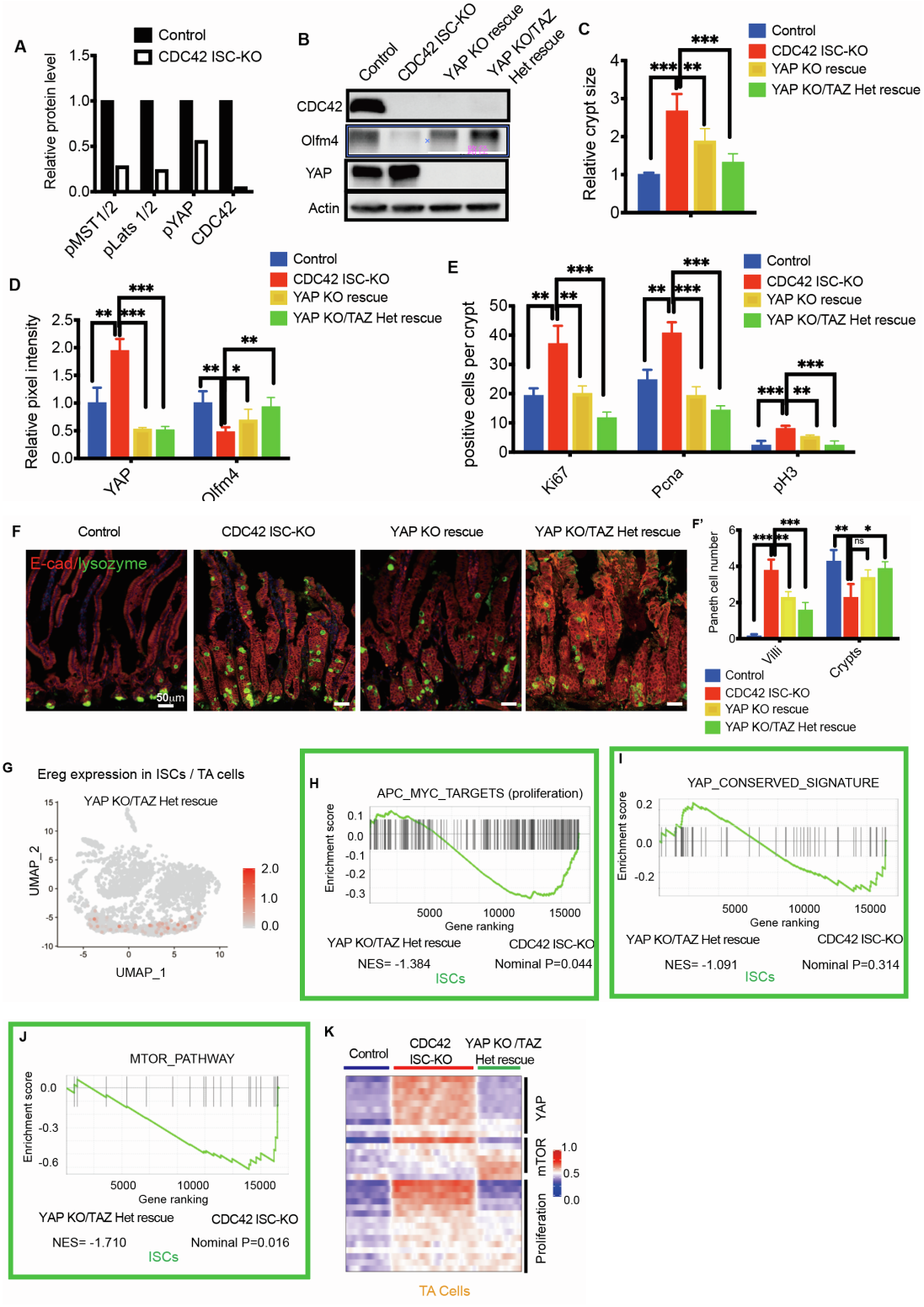

Supplemental Figure 4. YAP KO/TAZ Het reduces Ereg expression, cell proliferation, YAP and mTOR pathways in ISCs. **Related to Figure 4**

(A) Quantification of western blot in Fig. 4B.

(B) Western Blotting of CDC42 and Olfm4 in isolated small intestinal crypts.

(C) Quantification of H&E staining in Fig. 4F. Data are mean ± SD. ***p < 0.005.

(D, E) Quantification of immunofluorescent staining in Fig. 4G-K. Data are mean ± SD. *p < 0.05; **p < 0.01; ***p < 0.005.

(F) Representative images of immunofluorescent staining of duodenal sections and quantification: anti-E-cad (red), anti- lysozyme (green), and quantification of lysozyme immunofluorescent staining. Data are mean ± SD. *p < 0.05; **p < 0.01; ***p < 0.005; ns: not significant.

(G) Expression level of Ereg in YAP KO/TAZ Het rescue ISCs and TA cells.

(H-J) GSEA pathway enrichment map for proliferation, YAP and mTOR pathways in YAP KO/TAZ Het rescue ISC cluster.

(K) Heatmap of most-differentially altered genes in YAP pathway (10 genes), mTOR pathway (7 genes) and proliferation pathways (15 genes) in control, CDC42 ISC-KO, and YAP KO/TAZ Het rescue TA cell cluster. Columns, individual cells; rows, genes. n refers to gene numbers.

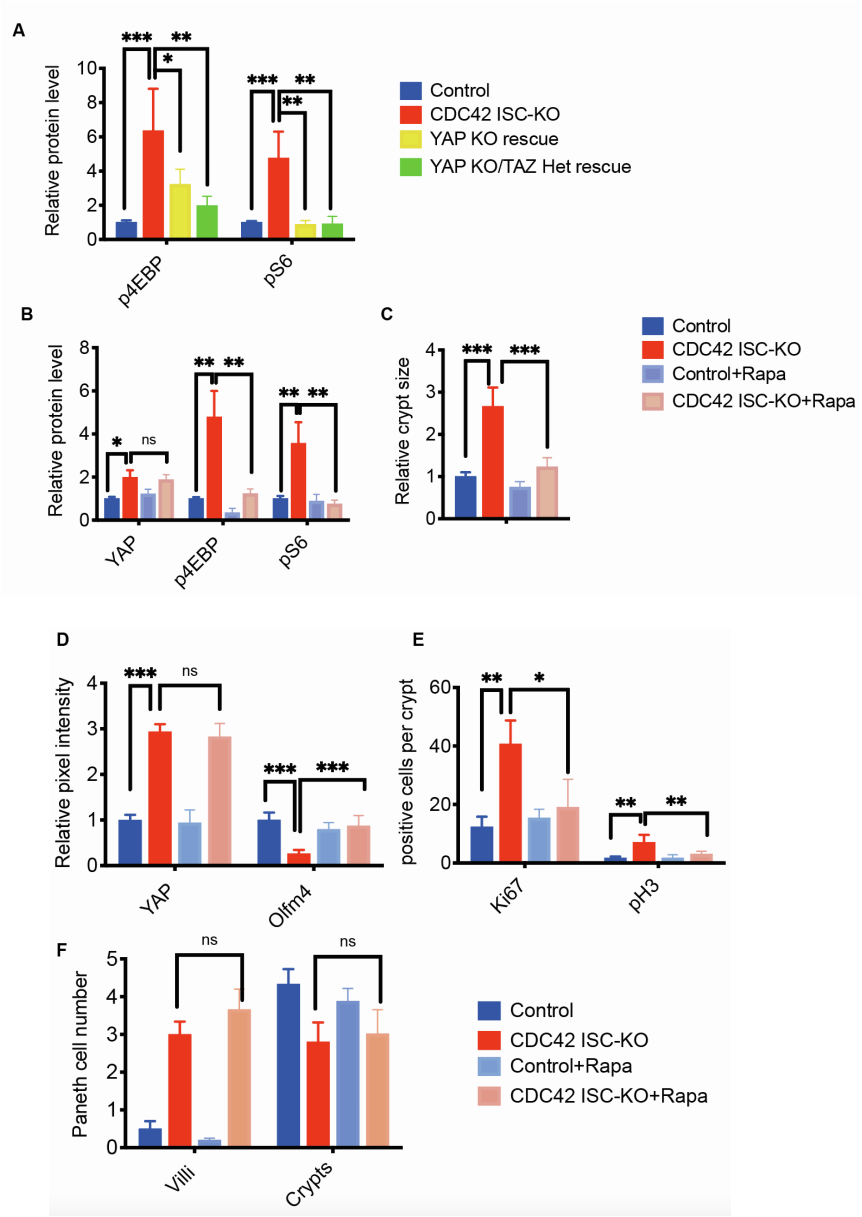

Supplemental Figure 5. Inhibition of mTOR signaling by rapamycin rescues ISCs and reduces TA cell population. **Related to Figure 5**

(A, B) Quantification of western blot in Fig. 5A, B. *p < 0.05; **p < 0.01; ***p < 0.005.

(C-F) Quantification of H&E and immunofluorescent staining in Fig. 5D-I. Data are mean ± SD. *p < 0.05; **p < 0.01; ***p < 0.005; ns: not significant.

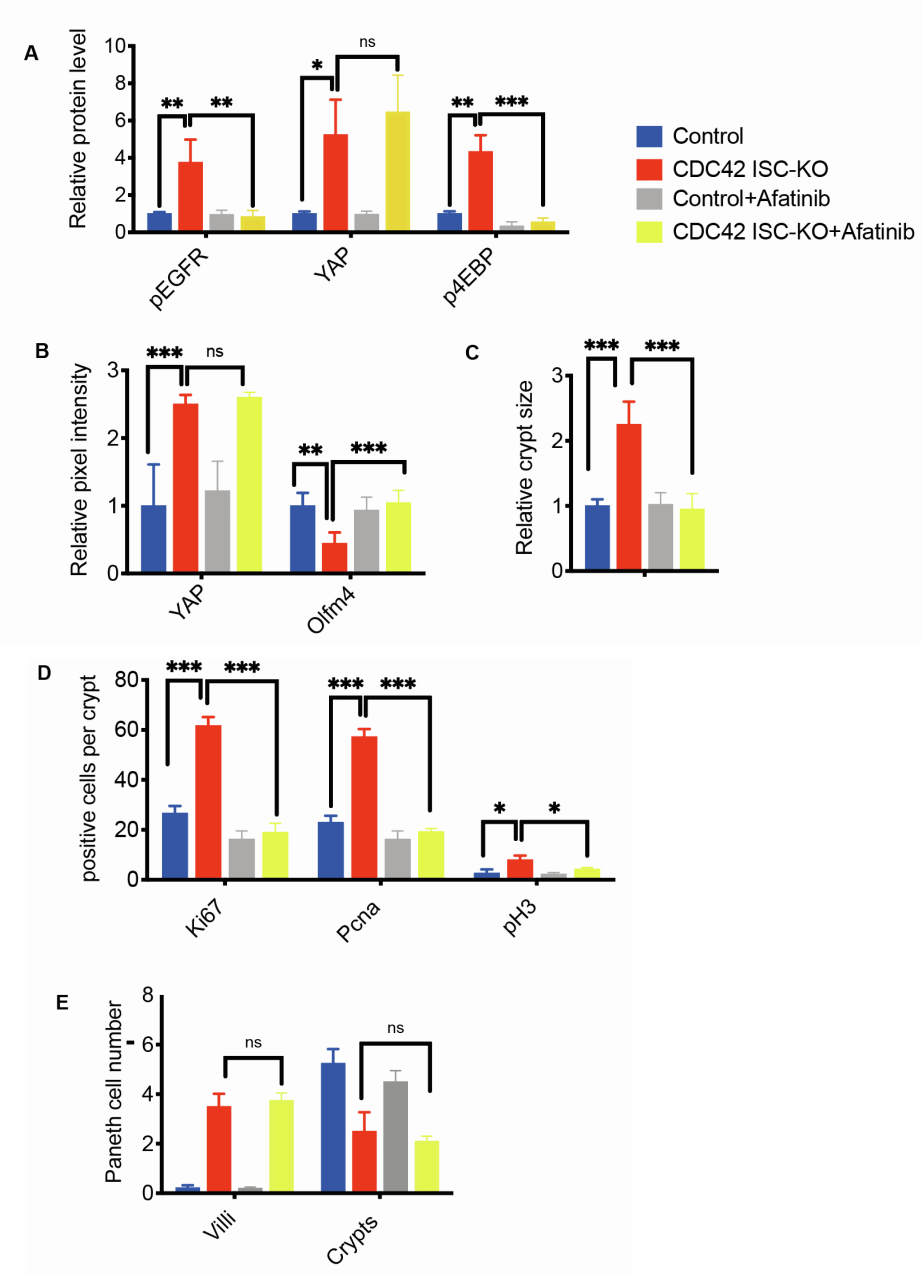

Supplemental Figure 6. Inhibition of Ereg by Afatinib rescues ISCs and reduces TA cell population. **Related to Figure 6**

(A) Quantification of western blot in Fig. 6A. *p < 0.05; **p < 0.01; ***p < 0.005; ns: not significant.

(B-E) Quantification of H&E and immunofluorescent in Fig. 6C-H. Data are mean ± SD. *p < 0.05; **p < 0.01; ***p < 0.005; ns: not significant.

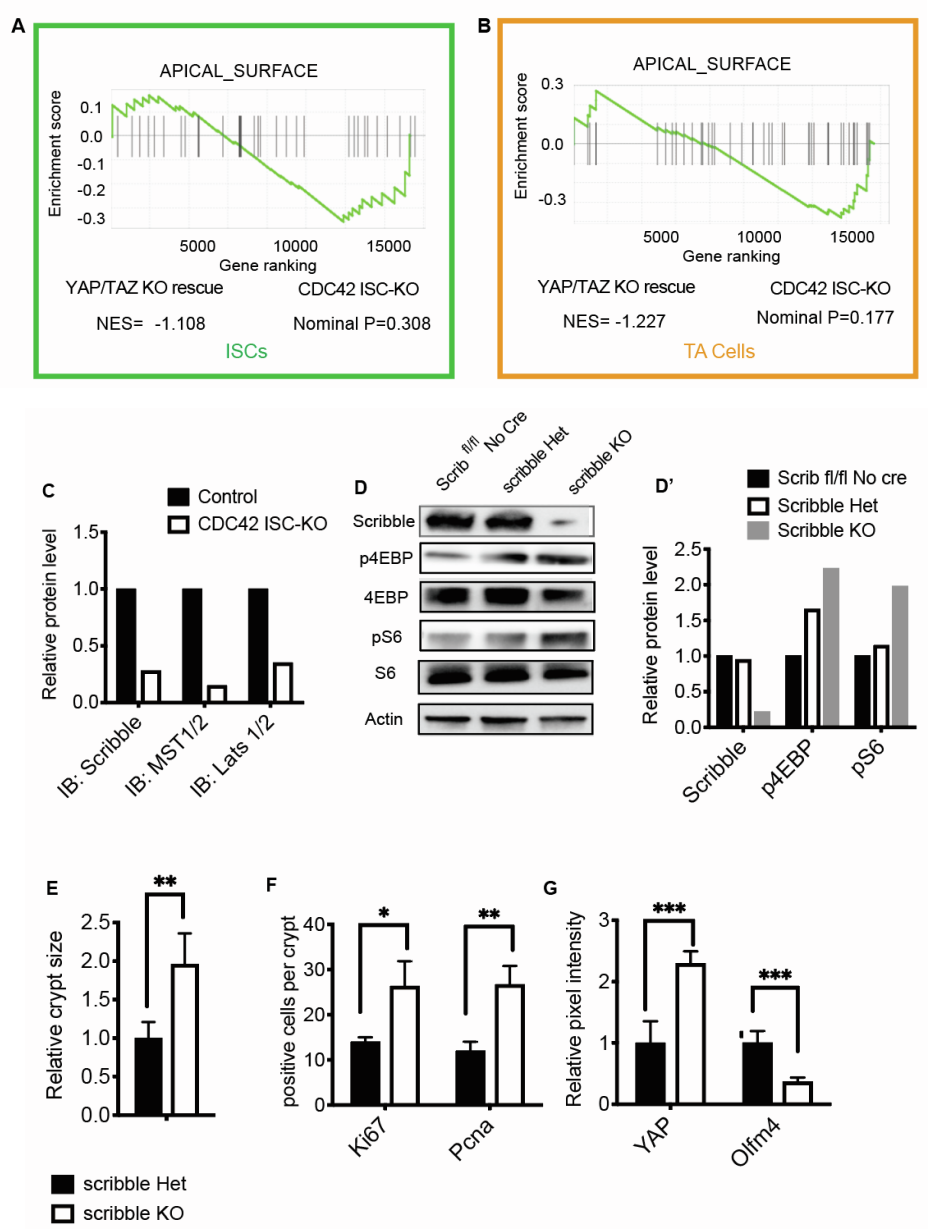

Supplemental Figure 7. Loss of CDC42 disrupts polarity, and loss of scribble crypts has elevated mTOR activity. **Related to Figure 7**

(A, B) GSEA pathway enrichment map for apical polarity pathways in YAP KO/TAZ Het rescue ISC and TA cell clusters.

(C) Quantification of western blot in Fig. 7D, E.

(D) Western Blotting of scribble, p4EBP, 4EBP, pS6, and S6 in in isolated small intestinal crypts, and quantification (representative of two independent repeats).

(E-G) Quantification of H&E and immunofluorescent staining in Fig. 7F-K. Data are mean ± SD. *$p < 0.05$; **$p < 0.01$; ***$p < 0.005$

Primers for qPCR		
ctgf:	Thermo Fisher	Mm01192933_g1
cyr61	Thermo Fisher	Mm00487499_g1
ereg	Thermo Fisher	Mm00514794_m1
cdc42	Thermo Fisher	Mm01194005_g1
beta-actin	Thermo Fisher	Mm02619580_g1
yap1	Thermo Fisher	Mm01143263_m1
taz	Thermo Fisher	Mm00504978_m1
lgr5	Thermo Fisher	Mm00438890_m1
olfm4	Thermo Fisher	Mm01320260_m1
ascl2	Thermo Fisher	Mm01268891_g1
pcna	Thermo Fisher	Mm00448100_g1
axin2	Thermo Fisher	Mm00443610_m1
cyclin D1	Thermo Fisher	Mm00432359_m1
mki67	Thermo Fisher	Mm01278617_m1
cdk4	Thermo Fisher	Mm00726334_s1
mcm5	Thermo Fisher	Mm00484840_m1
mcm6	Thermo Fisher	Mm00484848_m1

Supplemental Table 1 **Related to Key Resource Table**